ACADEMIC PRESS

Available online at www.sciencedirect.com

SCIENCE DIRECT®

Journal of Sound and Vibration 262 (2003) 1171–1189

JOURNAL OF SOUND AND VIBRATION

www.elsevier.com/locate/jsvi

Dynamic instability of stiffened plates subjected to non-uniform harmonic in-plane edge loading

A.K.L. Srivastava[a], P.K. Datta[a,*], A.H. Sheikh[b]

[a] *Department of Aerospace Engineering, Indian Institute of Technology, Kharagpur 721302, India*

[b] *Department of Ocean Engineering and Naval Architecture, Indian Institute of Technology, Kharagpur 721302, India*

Received 19 November 2001; accepted 1 July 2002

Abstract

The dynamic instability characteristics of stiffened plates subjected to in-plane partial and concentrated edge loadings are studied using finite element analysis. In the structural modelling, the plate and the stiffeners are treated as separate elements where the compatibility between these two types of elements is maintained. The method of Hill's infinite determinants is applied to determine the dynamic instability regions. Numerical results are presented to study the effects of various parameters, such as static load factor, aspect ratio, boundary conditions, stiffening scheme and load parameters on the principal instability regions of stiffened plates using Bolotin's method. The results show that location, size and number of stiffeners have a significant effect on the location of the boundaries of the principal instability region.

1. Introduction

Stiffened plates are structural components consisting of plates reinforced by a system of ribs to enhance their load-carrying capacities. These structures are widely used in aircraft, ship, bridge, building, and some other engineering activities. In many circumstances, these structures are exposed to dynamic loading. Stiffened plates are often designed to withstand a considerable in-plane load along with the transverse loads.

Two forms of buckling are usually considered. One possible mode is local buckling of the plate between the stiffeners, provided that the plate is reinforced with rigid stiffeners. In the second case, an overall buckling of the plate–stiffener combination. A considerably more economical design can be obtained if we permit simultaneous local and overall buckling at about the same

*Corresponding author. Fax: +3222-553-03.

E-mail address: pkdatta@aero.iitkgp.ernet.in (P.K. Datta).

0022-460X/03/$ - see front matter
doi:10.1016/S0022-460X(02)01094-5

stress level. The dynamic behaviour of stiffened plates subjected to uniform and non-uniform in-plane edge loading is of considerable importance to aerospace, mechanical and structural engineers. A structural element subjected to in-plane periodic forces may lead to parametric resonance, due to certain combinations of the load parameters. The instability may occur below the critical load of the structure under compressive loads over a range or ranges of excitation frequencies.

The Hill's method of infinite determinants is used for solving a system of Mathieu-type equation obtained in the present problem. The expansion of converging infinite determinants leads to a criterion to predict the stability properties of a finite number of coupled Mathieu equations. The dynamic instability of plates under periodic in-plane loads has been investigated by a number of researchers. For example, the dynamic stability of rectangular plates under various in-plane periodic forces has been studied by Bolotin [1], Jagdish [2] and Yamaki and Nagai [3]. The parametric instability characteristics of plates subjected to uniform harmonic loads have been studied by Hutt and Salam [4] using finite element method. Takahasi and Konishi [5] have studied the dynamic stability of a rectangular plate subjected to a linearly distributed load such as pure bending or a triangularly distributed load applied along the two opposite edges using harmonic balance method. The boundary conditions of the plate consisted of combination of simply supported edge and clamped edge. Unstable regions were presented for various boundary conditions of the plate and the loading conditions.

Deolasi and Datta [6] have studied the dynamic stability of thin, square, isotropic plates with simply supported boundary conditions, using finite element method where three degrees of freedom per node have been taken. Parametric instability characteristic of rectangular plates with localized damage subjected to in-plane periodic loading has been studied by Prabhakar and Datta [7].

The investigations on the parametric response of stiffened plates have been sparsely treated in the literature. Ambartsumyan and Khachaturian [8] have made the first attempt in the area of parametric instability of stiffened plates.

The onset of parametric resonance of a rectangular plate reinforced with closely spaced stiffeners has been studied by Duffield and Willems [9]. As stiffeners are thin-walled open members, the torsional rigidity of the stiffeners has not been taken into account. It was shown in their investigation that the principal regions of instability could significantly overlap for a stiffened plate. A similar study on skew stiffened plates was carried out by Merrit and Willems [10].

Mermertas and Belek [11] have employed the Galerkin method to investigate the dynamic stability of radially stiffened annular plates with both edges subjected to in-plane forces. Dynamic stability of laminated composite stiffened plates due to periodic in-plane forces at boundaries has been investigated by Liao and Cheng [12]. In most of the available results on dynamic instability of stiffened plates, the load has a uniform distribution over the edge. However, the applied load is seldom uniform and the boundary condition may completely be arbitrary in practice. The application of non-uniform loading on a structural component having general boundary conditions will alter the global quantities such as free vibration frequency, buckling load and dynamic instability region.

In the present study, the dynamic stability of a stiffened plate subjected to various in-plane uniform and non-uniform, including partial and concentrated edge loadings, is investigated. The

effects of various parameters like static and dynamic load factors, aspect ratio, boundary conditions, percentage of loaded length and position of point loading on the instability behaviour of stiffened plate are examined.

In the present analysis, the plate is modelled with nine-noded isoparametric quadratic element where the contributions of bending and membrane actions are taken into account. One of the advantages of the element is that it includes the effect of shear deformation and rotary inertia in its formulation. Thus, the analysis can be carried out for both thin and thick plates. Moreover, it can be applied to a structure having irregular boundaries with some modifications. The formulation of the stiffener is done in such a manner that it may lie anywhere within a plate element [13]. In order to maintain compatibility between the plate and the stiffener, the interrelation functions used for the plate are used for the stiffeners also.

2. Theory and formulations

The basic configuration of the problem considered here is a stiffened plate as shown in Fig. 1, subjected to various non-uniform harmonic in-plane edge loadings.

2.1. Governing equations

The equation of equilibrium for an elastic system undergoing small displacements at the instant of buckling may be written in matrix form as

$$[M]\{\ddot{q}\} + [[K_e] - P[K_G]]\{q\} = 0. \tag{1}$$

In the above equation, the in-plane load factor $P(t)$ is periodic and can be expressed in the form

$$P(t) = P_S + P_t \cos \Omega t, \tag{2}$$

where P_S is the static portion of $P(t)$, P_t is the amplitude of the dynamic portion of $P(t)$ and Ω is the frequency of excitation. The static buckling load P_{cr} may be used to express P_S and P_t as

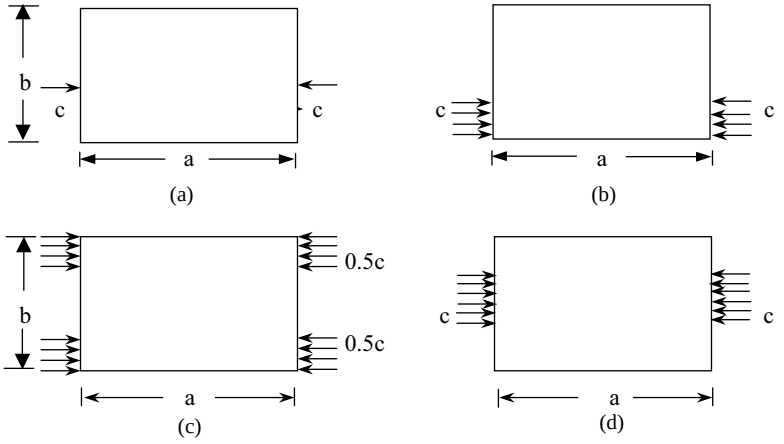

Fig. 1. Description of the problem, i.e., various loading cases.

follows:

$$P_S = \alpha P_{cr}, \quad P_t = \beta P_{cr}, \tag{3}$$

where α and β are static and dynamic load factors, respectively. Using Eqs. (2) and (3), the equation of motion (1) may be expressed as

$$[M]\{\ddot{q}\} + [[K_e] - \alpha P_{cr}[K_G] - \beta P_{cr}[K_G]\cos \Omega t]\{q\} = 0. \tag{4}$$

Eq. (4) represents a system of second order differential equation with periodic coefficients of Mathieu–Hill type. The boundaries of dynamic instability are formed by the periodic solution of period T and $2T$, where $T = 2\pi/\Omega$. The boundaries of the primary instability region with period $2T$ are of practical importance and the solution can be achieved in the form of trigonometric series:

$$q(t) = \sum_{k=1,3,5}^{\infty} \left[\{a\}_k \sin\frac{k\Omega t}{2} + \{b\}_k \cos\frac{k\Omega t}{2} \right]. \tag{5}$$

After substitution of the above equation into Eq. (4), if the first term of the series is considered (equating coefficients of $\sin(\Omega t/2)$ and $\cos(\Omega t/2)$), it leads to a series of algebraic equations for the determination of instability regions. Principal instability region, which is of practical importance, corresponds to $k = 1$ and for this case, the instability equation leads to

$$\left[[K_e] - \alpha P_{cr}[K_G] \pm \tfrac{1}{2}\beta P_{cr}[K_G] - \frac{\Omega^2}{4}[M] \right]\{q\} = 0. \tag{6}$$

The two conditions under plus and minus signs correspond to two boundaries of the dynamic instability region. The eigenvalues give the value of $_{\Omega}$, which are the bounding frequencies of the instability regions for the given values of α and β.

2.2. Finite element formulation

The plate skin and the stiffeners are modelled as separate elements but the compatibility between them is maintained. The element matrices of the stiffened plate element consist of the contribution of the plate and that of the stiffener. The effect of in-plane deformations is taken into account in addition to the deformations due to bending, which will help to model the stiffener eccentricity conveniently. This is similar to the concept proposed by Sheikh and Mukhopadhyay [14] and Mukherjee and Mukhopadhyay [13,15]. The stiffness matrix of the plate and that of the stiffener have been discussed in detail in Refs. [13,15] where they have used eight-noded isoparametric element and as such will be discussed here rather briefly by giving the important expressions directly in their final form in order to avoid repetition.

The nine-noded isoparametric quadratic element with five degrees of freedom (u, v, w, θ_x, and θ_y) per node is employed in the present analysis. The co-ordinates at a point within the element are approximated in terms of its nodal co-ordinates [16]. The shape functions are expressed in terms of non-dimensional parameters ξ and η. In order to correlate the axis system ($x-y$) with (ξ–η), the Jacobian matrix |J| and its inverse may be used [16].

2.2.1. Plate element formulation

The elastic stiffness matrix $[K_P]$, geometric stiffness matrix $[K_{GP}]$ and mass matrix $[M_P]$ of the plate element may be expressed as follows:

$$[K_P] = \int_{-1}^{+1} \int_{-1}^{+1} [B_P]^{\mathrm{T}} [D_P][B_P] |\mathrm{J}_P| \, \mathrm{d}\xi \, \mathrm{d}\eta, \tag{7}$$

$$[K_{GP}] = \int_{-1}^{+1} \int_{-1}^{+1} [B_{GP}]^{\mathrm{T}} [\sigma_P][B_{GP}] |\mathrm{J}_P| \, \mathrm{d}\xi \, \mathrm{d}\eta, \tag{8}$$

$$[M_P] = \int_{-1}^{+1} \int_{-1}^{+1} [N]^{\mathrm{T}} [m_P][N] |\mathrm{J}_P| \, \mathrm{d}\xi \, \mathrm{d}\eta, \tag{9}$$

where

$$[B_P] = [[B_P]_1 \;\; [B_P]_2 \;\; \cdots \;\; [B_P]_r \;\; \cdots \;\; [B_P]_9], \tag{10}$$

$$[B_{GP}] = [[B_{GP}]_1 \;\; [B_{GP}]_2 \;\; \cdots \;\; [B_{GP}]_r \;\; \cdots \;\; [B_{GP}]_9], \tag{11}$$

and

$$|\mathrm{J}_P| = |\mathrm{J}|. \tag{12}$$

The different matrices in the above equations may be written as follows:

$$[B_{GP}]_r = \begin{bmatrix} 0 & 0 & \dfrac{\partial N_r}{\partial x} & 0 & 0 \\ 0 & 0 & \dfrac{\partial N_r}{\partial y} & 0 & 0 \\ 0 & 0 & 0 & \dfrac{\partial N_r}{\partial x} & 0 \\ 0 & 0 & 0 & 0 & \dfrac{\partial N_r}{\partial y} \\ 0 & 0 & 0 & 0 & \dfrac{\partial N_r}{\partial x} \\ 0 & 0 & 0 & \dfrac{\partial N_r}{\partial y} & 0 \end{bmatrix}, \tag{13}$$

$$[B_p]_r = \begin{bmatrix} \frac{\partial N_r}{\partial x} & 0 & 0 & 0 & 0 \\ 0 & \frac{\partial N_r}{\partial y} & 0 & 0 & 0 \\ \frac{\partial N_r}{\partial y} & \frac{\partial N_r}{\partial x} & 0 & 0 & 0 \\ 0 & 0 & 0 & -\frac{\partial N_r}{\partial x} & 0 \\ 0 & 0 & 0 & 0 & -\frac{\partial N_r}{\partial y} \\ 0 & 0 & 0 & -\frac{\partial N_r}{\partial y} & -\frac{\partial N_r}{\partial x} \\ 0 & 0 & \frac{\partial N_r}{\partial x} & -N_r & 0 \\ 0 & 0 & \frac{\partial N_r}{\partial y} & 0 & -N_r \end{bmatrix}, \tag{14}$$

$$[\sigma_P] = \begin{bmatrix} \sigma_x t & \tau_{xy} t & 0 & 0 & 0 & 0 \\ \tau_{xy} t & \sigma_y t & 0 & 0 & 0 & 0 \\ 0 & 0 & \frac{\sigma_x t^3}{12} & 0 & \frac{\tau_{xy} t^3}{12} & 0 \\ 0 & 0 & 0 & \frac{\sigma_y t^3}{12} & 0 & \frac{\tau_{xy} t^3}{12} \\ 0 & 0 & \frac{\tau_{xy} t^3}{12} & 0 & \frac{\sigma_x t^3}{12} & 0 \\ 0 & 0 & 0 & \frac{\tau_{xy} t^3}{12} & 0 & \frac{\sigma_y t^3}{12} \end{bmatrix} \tag{15}$$

and

$$[m_P] = \begin{bmatrix} \rho t & 0 & 0 & 0 & 0 \\ 0 & \rho t & 0 & 0 & 0 \\ 0 & 0 & \rho t & 0 & 0 \\ 0 & 0 & 0 & \frac{\rho t^3}{12} & 0 \\ 0 & 0 & 0 & 0 & \frac{\rho t^3}{12} \end{bmatrix}. \tag{16}$$

2.2.2. Stiffener element formulation

The elastic stiffness matrix $[K_S]$, geometric stiffness matrix $[K_{GS}]$ and mass matrix $[M_S]$ of a stiffener element placed anywhere within a plate element and oriented in the direction of x may be

expressed, in a manner similar to those of the plate element, as follows:

$$[K_S] = \int_{-1}^{+1} [B_S]^{\mathrm{T}} [D_S][B_S] |\mathrm{J}_S| \, \mathrm{d}\xi, \tag{17}$$

$$[K_{GS}] = \int_{-1}^{+1} [B_{GS}]^{\mathrm{T}} [\sigma_S][B_{GS}] |\mathrm{J}_S| \, \mathrm{d}\xi \tag{18}$$

and

$$[M_S] = \int_{-1}^{+1} [N]^{\mathrm{T}} [m_S][N] |\mathrm{J}_S| \, \mathrm{d}\xi, \tag{19}$$

where

$$[B_S] = \big[[B_S]_1 \;\; [B_S]_2 \;\; \cdots \;\; [B_S]_r \;\; \cdots \;\; [B_S]_9\big], \tag{20}$$

$$[B_{GS}] = [[B_{GS}]_1 \;\; [B_{GS}]_2 \;\; \cdots \;\; [B_{GS}]_r \;\; \cdots \;\; [B_{GS}]_9] \tag{21}$$

and $|\mathrm{J}_S|$ is the Jacobian of the stiffener, which is one-half of its actual length within an element.

The different matrices in the above equations may be written as follows:

$$[B_S]_r = \begin{bmatrix} \dfrac{\partial N_r}{\partial x} & 0 & 0 & 0 & 0 \\ 0 & 0 & 0 & -\dfrac{\partial N_r}{\partial x} & 0 \\ 0 & 0 & 0 & 0 & \dfrac{\partial N_r}{\partial x} \\ 0 & 0 & \dfrac{\partial N_r}{\partial x} & -N_r & 0 \end{bmatrix}, \tag{22}$$

$$[D_S] = \begin{bmatrix} EA_S & EF_S & 0 & 0 \\ EF_S & EI_S & 0 & 0 \\ 0 & 0 & GT_S & 0 \\ 0 & 0 & 0 & GA_S/1.2 \end{bmatrix}, \tag{23}$$

$$[B_{GS}] = \begin{bmatrix} 0 & 0 & \dfrac{\partial N_r}{\partial x} & 0 & 0 \\ 0 & 0 & 0 & \dfrac{\partial N_r}{\partial x} & 0 \end{bmatrix}, \tag{24}$$

$$[\sigma_S] = \begin{bmatrix} \sigma_x A_S & 0 \\ 0 & \sigma_x I_S \end{bmatrix} \tag{25}$$

and

$$[m_S] = \rho \begin{bmatrix} A_S & 0 & 0 & 0 & 0 \\ 0 & A_S & 0 & 0 & 0 \\ 0 & 0 & A_S & 0 & 0 \\ 0 & 0 & 0 & F_S & 0 \\ 0 & 0 & 0 & 0 & P_S \end{bmatrix}, \tag{26}$$

where A_S is the area, F_S is the first moment of area about a reference plane, I_S is the second moment of area about the reference plane, T_S is the torsional constant and P_S is the polar moment of area of the stiffener cross-section.

For the stiffeners placed in the direction of y, the formulation will be similar with appropriate changes for the co-ordinate variables.

A computer program is developed to perform all the necessary computations. The geometric stiffness matrix is essentially a function of the in-plane stress distribution in the element due to applied edge loading. Since the stress field is non-uniform, for a given edge loading and boundary conditions, the static equation, i.e., $[K]\{\delta\} = \{F\}$ is solved to get these stresses. The geometric stiffness matrix is now constructed with the known in-plane stresses. The computer program developed accepts two sets of boundary conditions, one for the static analysis and the other for the buckling analysis. In the present case, a three-point integration scheme is adopted for the evaluation of all the matrices except the portion of the stiffness matrix related to shear strain components.

The overall elastic stiffness matrix, geometric stiffness matrix and mass matrix are generated from the assembly of those element matrices and stored in a single array where the variable bandwidth profile storage scheme is used. The solution of eigenvalues is performed by the simultaneous iteration technique proposed by Corr and Jennings [17].

3. Results and discussions

3.1. Convergence and validation

In a finite element analysis, it is desirable to have the convergence studies to estimate the order of mesh size necessary for the numerical solution. For this purpose, a simply supported and clamped rectangular plate subjected to concentrated in-plane edge loading as shown in Fig. 1(a) is analyzed with various mesh sizes taking $c/b = 0.5$ and aspect ratio (a/b) of 1.0, 2.0.and 0.5. Results obtained in the form of buckling load parameters are presented in Table 1 with those of Leissa and Ayoub [18] and Brown [19], which show good agreement. As the convergence study shows that a mesh size of 10×10 is sufficient enough to get a reasonable order of accuracy, the analysis in the subsequent problems is carried out with this mesh size.

For the validation of buckling load parameter of stiffened plates subjected to partially distributed in-plane edge loading, as shown in Fig. 1(b), the analysis is carried out for $c/b = 1$. Actually, this corresponds to a fully loaded plate problem, for which analytical, finite element and other solutions are available in the literature. In the present case, the plate contains one stiffener

Table 1
Convergence and comparison of buckling load parameter ($\lambda = P_{cr}b/D$) of a simply supported rectangular plate under concentrated edge loading (Fig. 1)

c/b	Boundary condition	a/b	Buckling load parameter (λ)						
			Present					Leissa [18]	Brown[19]
			4×4	6×6	8×8	10×10	12×12		
0.5	SSSS	1	26.84	26.81	26.76	26.62	26.61	25.81	25.44
		2	29.78	29.56	29.45	29.30	29.31	28.52	28.27
		0.5	31.23	31.17	31.15	31.06	30.06	30.06	29.53
	CCCC	1	66.13	66.21	66.56	66.66	66.70	—	67.23
		2	63.23	63.34	63.71	63.79	63.81	—	65.03
		0.5	80.78	80.56	81.23	81.04	81.12	—	82.30

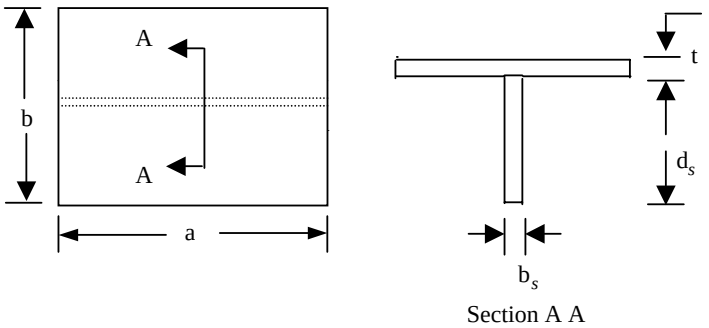

Fig. 2. Stiffened plate cross-section

Table 2
Validation of buckling load parameter of a simply supported stiffened plates under distributed in-plane edge loading ($c/b = 1$)

Buckling load parameter (λ)						
A_S/bt	EI_S/bD					
	5		10		15	
	Ref. [13]	Present	Ref. [13]	Present	Ref. [20]	Present
0.05	12.0	12.62	16.0	15.99	16.0	15.998
0.1	11.10	12.39	16.0	15.99	16.0	15.995

as shown in Fig. 2. By varying the stiffener parameters, the plate is analyzed taking $a/b = 1.0$ (Fig. 2) and simply supported boundary condition at the four edges. Results obtained in the present analysis are presented with the analytical solution of Timoshenko and Gere [20] and finite element results of Mukherjee and Mukhopadhyay [13] in Table 2. It shows that the agreement between the results obtained from different sources is very good.

Table 3
Comparison of principal regions of instability of a simply supported square plate subjected to uniform in-plane edge loading (uni-axial) for different static load factors (α)

Excitation frequency parameter									
α= 0					α= 0.6				
β	Present		Ref. [4]		β	Present		Ref. [4]	
	U	L	U	L		U	L	U	L
0	39.46	39.46	39.46	39.46	0	25.04	25.04	25.06	25.06
0.4	43.16	35.37	43.00	35.32	0.16	27.41	22.48	27.43	22.49
0.8	46.54	30.73	46.56	30.78	0.32	29.58	19.51	29.60	19.53
1.2	49.54	24.02	49.52	25.06	0.48	31.55	15.89	31.57	15.91

For the validation of dynamic instability, a similar approach may be adopted, i.e., the value of c/b may be taken as 1.0 for a uniformly distributed partial in-plane edge loading. In this case, a simply supported square plate is analyzed with different static and dynamic load factors. The boundary frequencies obtained in the present analysis are presented with those of Hutt and Salam [4] in Table 3, which show good agreement.

3.2. *In-plane stress distribution under non-uniform loading*

Plates subjected to non-uniform in-plane loading may develop non-uniform stress distribution which may considerably influence the stability behaviour of the plates. Hence, it is customary to study the nature of in-plane stress distribution under non-uniform loading, prior to subsequent analysis. Figs. 3 and 4 show the non-dimensional in-plane stresses $\sigma_x at/P$ and $\sigma_y at/P$ for a square plate subjected to a pair of concentrated edge loading on two opposite edges at various locations. It can be observed from Fig. 3 that for concentrated compressive loading at the ends of two opposite edges, a substantial compressive zones exists over some localized area which lies near the line of action of the forces, i.e., near the edge $x = 0$. In compressive zones, the stresses are predominantly in the direction of loading. When the compressive loading is shifted to the centre of the edges, the compressive zones is spread over almost entire plate area, but the stresses are considerably higher in a zone near to the centre of the plate as shown in Fig. 4. Again, the in-plane stress distribution and the influence of edge restraints in the substantial compressive zones play a role in the observed buckling behaviour. Thus, the dynamic stability behaviour of the plates under concentrated and patch types of loading would be of considerable interest.

3.3. *Effect of different parameters on dynamic instability of stiffened plates*

The effect of different parameters on dynamic instability region of stiffened plates is studied in this section. It includes the location and the extent of edge loading, static and dynamic load factors, plate aspect ratio, boundary conditions, number of stiffeners, location of the stiffeners, and stiffener geometric parameters. The study is made for different types of edge loading as shown in Fig. 1. Results are presented in graphical form where the instability region is shown by the

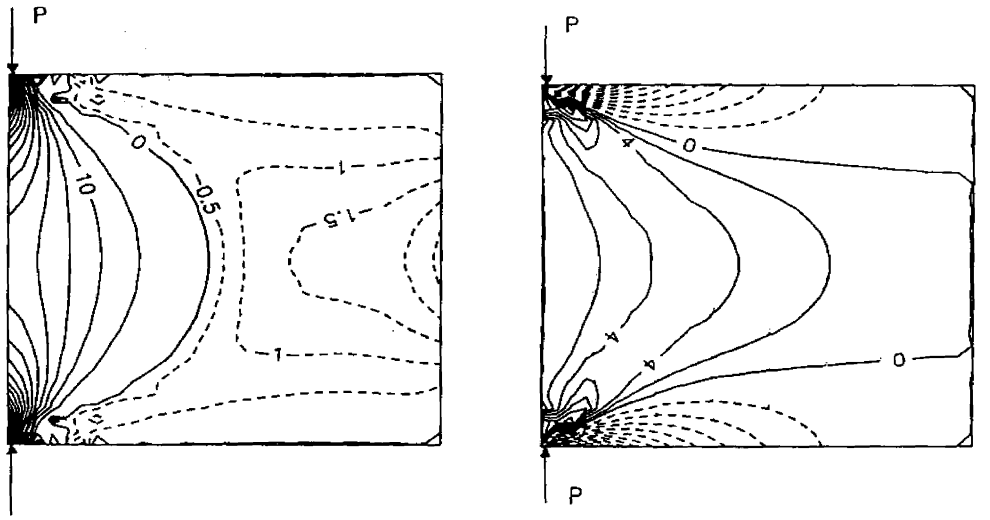

(a) Non-domensional in-plane stress distribution (σ_y *at*/*P*) (b) Non-domensional in-plane stress distribution (σ_x *at*/*P*)

Fig. 3. Non-dimensional in-plane stress distributions under a pair of concentrated loading at one end of two opposite edges.

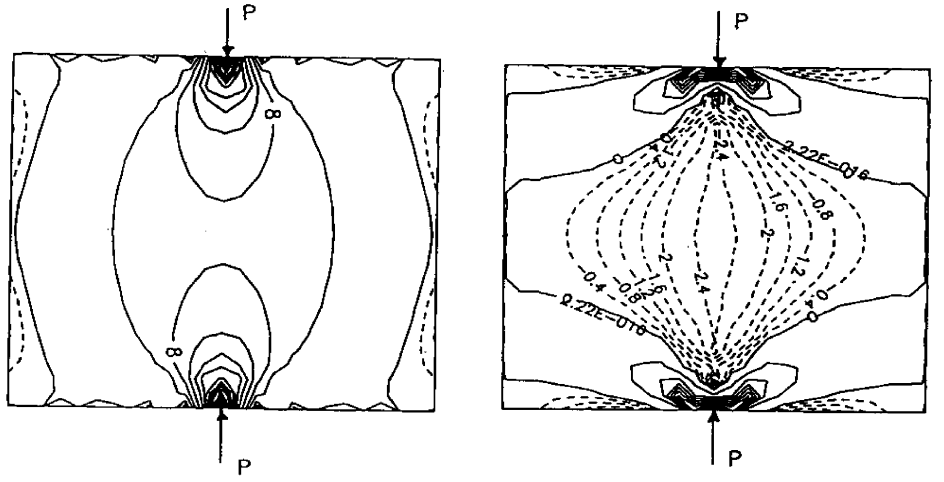

(a) Non-domensional in-plane stress distribution (σ_y *at*/*P*) (b) Non-domensional in-plane stress distribution (σ_x *at*/*P*)

Fig. 4. Non-dimensional in-plane stress distributions under a pair of concentrated loading at the centre of two opposite edges.

upper and lower values of the non-dimensional excitation frequency parameter ($\Omega = \bar{\Omega}a^2\sqrt{\rho h/D}$). In all these cases, the frequency parameter is plotted against dynamic load factor (β) for different values of the parameters as mentioned above.

3.3.1. Concentrated edge loading

The case of concentrated edge loading as shown in Fig. 1(a) is considered in this section.

As a first case, the effect of position of the concentrated load on the region of dynamic instability of the stiffened plate is studied by taking different values of c/b ratio. The plate is simply supported at its four edges and the data used for its geometry are $a = 600\,\text{mm}$, $b = 600\,\text{mm}$, $t = 6.33\,\text{mm}$, $b_s = 12.7$ and $d_s = 22.2\,\text{mm}$. Taking a static load factor (α) of 0.2, the plate is analyzed and the results obtained are presented in Fig. 5. The figure shows that the instability region and its width depend on the position of the concentrated load. It is observed that the width of instability regions is reduced with decrease in value of c/b ratio. Again it is found that the instability occurs at higher excitation frequencies when the load is closer to the support. These effects are due to the restraint imposed by the edge support. In this study, the dynamic load factor (β) is varied from 0 to 0.8. In the higher range of β ($\geqslant 0.4$), the upper excitation frequency parameter for higher c/b ratio is interestingly found to be comparable with that corresponding to lower c/b ratio. For lower values of β, the pattern is just opposite. This behaviour of stiffened plate is distinctly different from that of corresponding unstiffened plate results available in the literature [6]. In the case of the stiffened plate problem considered here, the change of pattern in the range of higher dynamic load factor (β) is due to the restraint imposed by the stiffener.

The effect of static load factor (α) on the dynamic instability region of the stiffened plate considered above is studied for load position, $c/b = 0.2$ in all the cases. Results for $\alpha = 0.2$, 0.4, 0.6, and 0.8 are presented in Fig. 6. It shows that the instability region is shifted to lower frequencies and becomes wider with the increase of static load factor (α).

In order to study the effect of aspect ratio (a/b) of a stiffened plate on its dynamic instability behaviour, the length (a) of the stiffened plate considered above is varied keeping the other parameters unchanged. The analysis is carried out taking $c/b = 0.2$ and $\alpha = 0.2$ in all the cases. The investigation is made for $a/b = 0.5$, 1.0, 1.5 and 2.0, which is shown in Fig. 7. It is observed that the onset of dynamic instability occurs at higher frequencies for higher aspect ratios (a/b). The instability region is also found to be broader with the increase in aspect ratio (a/b).

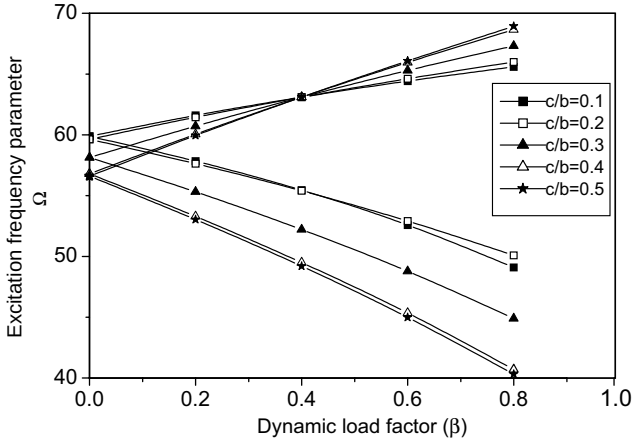

Fig. 5. Effect of position of load on instability region of simply supported stiffened plate subjected to in-plane concentrated load $\alpha = 0.2$.

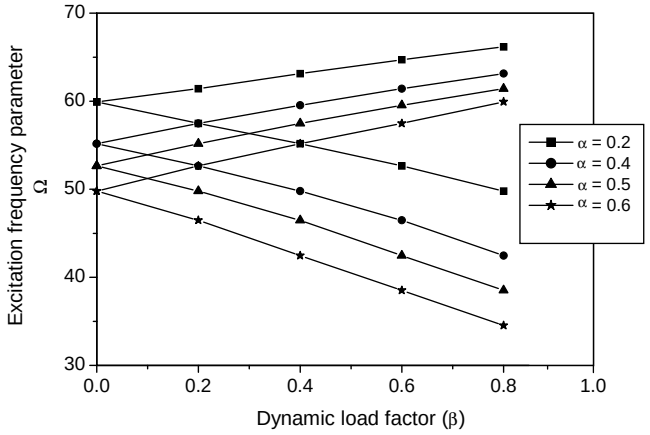

Fig. 6. Effect of static load factor on instability region of simply supported stiffened plate subjected to in-plane concentrated load ($c/b = 0.2$).

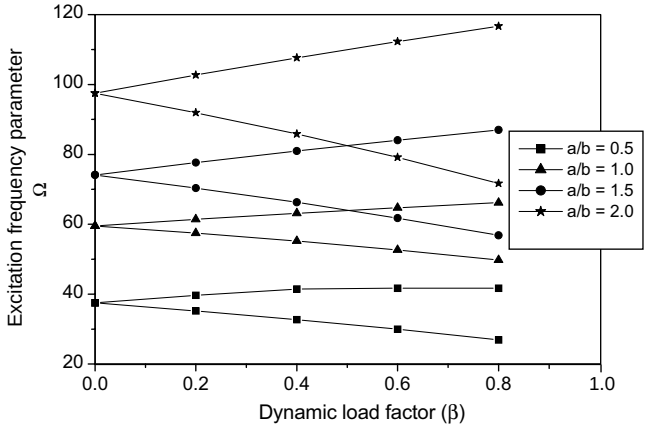

Fig. 7. Effect of aspect ratio on instability region of simply supported stiffened plate subjected to in-plane concentrated load ($c/b = 0.2$, $\alpha = 0.2$).

The effect of boundary conditions (SSSS, CCCC, SCSC) on the dynamic instability regions of unstiffened and stiffened plates are shown in Fig. 8 taking $c/b = 0.2$ and $\alpha = 0.2$ for the loading condition (Fig. 1(a)). It is observed that the excitation frequency of the plate reinforced with stiffener is more than that without stiffener for all edge conditions. It is also observed that the instability occurs at a higher excitation frequency for clamped edge condition than simply supported, which is due to the restraint at the edges. The width of the instability region also decreases with the increase of restraint at the edges for both unstiffened and stiffened plates.

The effect of varying number of stiffeners on the principal dynamic instability regions of the stiffened plate subjected to in-plane concentrated load is shown in Fig. 9. The analysis is done for one central stiffener, two equispaced stiffeners and three-equispaced stiffeners parallel to x-axis. Plate and stiffener dimensions are the same as before. Further, each stiffener cross-section is

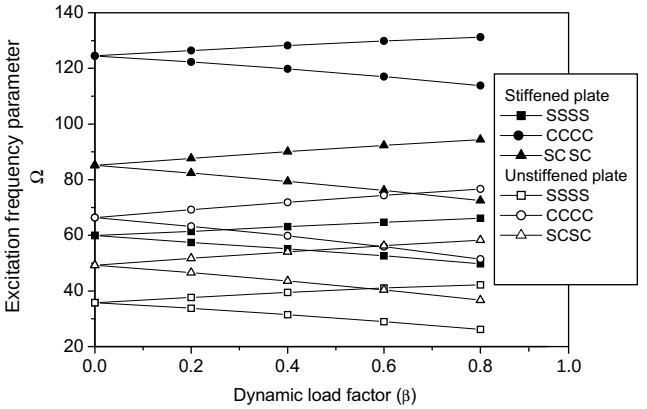

Fig. 8. Effect of boundary condition on instability region of stiffened plate subjected to in-plane concentrated load ($c/b = 0.2$, $\alpha = 0.2$).

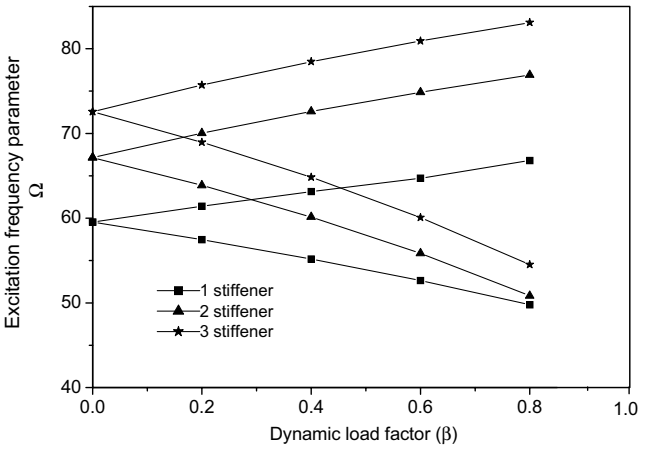

Fig. 9. Effect of number of stiffeners on instability region of simply supported stiffened plate subjected to in-plane concentrated load ($c/b = 0.2$, $\alpha = 0.2$).

similar. It is observed from Fig. 9 that the value of the boundary frequency parameter increases as the number of stiffener increases.

3.3.2. *Partial edge loading at one end*

The case of partial edge loading at one end as shown in Fig. 1(b) is considered in this section.

The effect of load bandwidth (Fig. 1(b)) on the region of dynamic instability of the stiffened plate is studied. The plate is simply supported at its four edges and the data used for its geometry are the same as in the earlier case. Taking static load factor (α) of 0.2 and different values of c/b ratio ($c/b = 0.1$, 0.2, 0.4, 0.5, 0.6, 0.8 and 1.0), the plate is analyzed and the results obtained are presented in Fig. 10. The figure shows that the instability region and its width depend on the positions of the partial edge load at one end. It is observed that for small value of c/b (0.2), the widths of the dynamic instability regions are usually smaller in comparison to those for c/b close

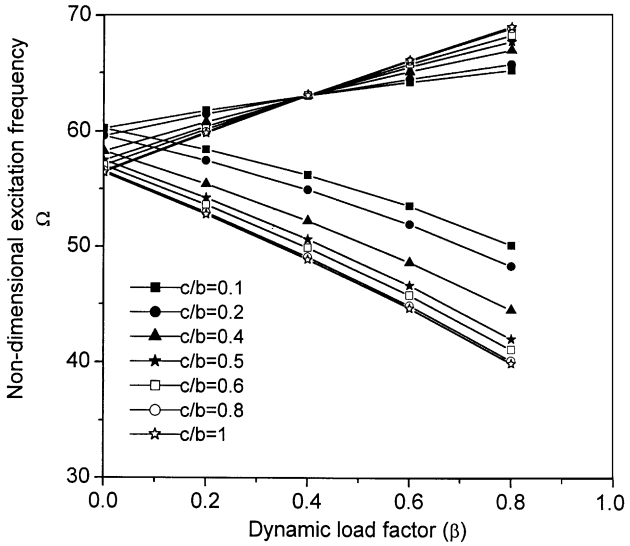

Fig. 10. Effect of load bandwidth on instability region of simply supported stiffened plate subjected to in-plane partial loading at one end ($\alpha = 0.2$).

to unity ($c/b = 0.8$). This is because of the fact that the restraint of the edge has a stabilizing effect on the dynamic instability behaviour of the stiffened plate for small bandwidth of loading. It is also observed that, the instability occurs at lower excitation frequencies with the increase of distance from the edges (c/b). In this study, the dynamic load factor (β) is varied from 0 to 0.8. It is observed that the nature of upper excitation frequency parameter with c/b ratio is similar to that of concentrated loading case. In the case of the stiffened plate problem considered here, the change of pattern in the range of higher dynamic load factor (β) is due to the presence of stiffener at the centre. The effect of static load factor, boundary condition, aspect ratios and varying number of stiffeners on the instability regions are studied and it has been observed that the results are similar to those of in-plane concentrated load case discussed earlier.

3.3.3. *Partial edge loading at both ends*

The case of partial edge loading at both ends as shown in Fig. 1(c) is considered in this section.

The effect of load bandwidth ($c/b = 0.2$, 0.4, 0.6, 0.8, 1.0) on instability region of simply supported square plate with one central stiffener is studied. The non-dimensionalized static part of the in-plane force, α, is 0.2 and the results obtained are presented in Fig. 11. It is observed that the instability region and its width depend on the positions of load bandwidth. It may be observed from Fig. 11 that for small value of c/b (0.2), the widths of the instability zones are smaller as compared to those for c/b close to unity ($c/b = 0.8$). This means that the plate is less susceptible to dynamic instability for band loading near the edges. This is because of the edge restraining effects.

Again it is observed that the nature of upper excitation frequency parameter with c/b ratio is similar to that of previous loading cases.

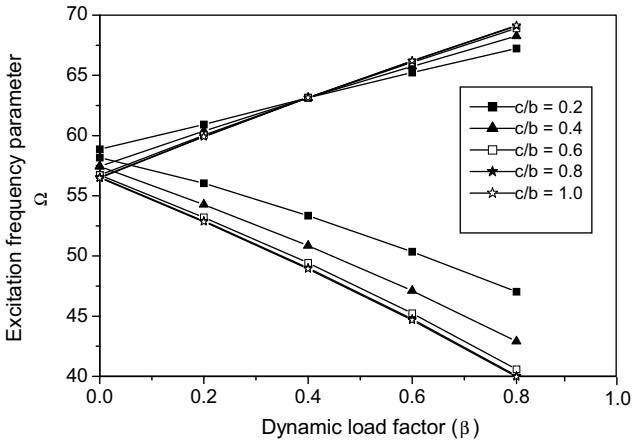

Fig. 11. Effect of load bandwidth on instability region of simply supported stiffened plate subjected to partial edge loading at both ends ($\alpha = 0.2$).

3.3.4. *Partial edge loading at the centre*

The case of partial edge loading at the centre as shown in Fig. 1(d) is considered in this section. The effects of static load factor, boundary condition, aspect ratios and varying number of stiffeners on the instability regions are studied. It is observed that the results obtained are similar to those of other loading cases.

The stiffener parameter terms δ and γ are defined as $\delta = A_S/bt$ =ratio of cross-sectional area of the stiffener to the plate area, where A_S is the area of the stiffener and $\gamma = EI_S/bD$ =ratio of bending stiffness rigidity of stiffener to that of the plate, where I_S is the moment of inertia of the stiffener cross-section about reference axis.

The effects of stiffener area ratio and bending stiffness rigidity ratio of stiffener on the dynamic stability of stiffened plate are of interest.

A simply supported square plate with a central stiffener has been analyzed with various rigidities of the stiffener. The ratio of the bending stiffness (EI_s/bD) has been varied from 5 to 20. The torsional inertia of the stiffeners has been neglected. The effect of bending stiffness rigidity of the stiffened plate with one central stiffener, having fixed stiffener area ratio (say $\delta = 0.1$), on the principal dynamic stability region is shown in Fig. 12. It is observed that if δ is fixed and γ is increased, the instability boundary frequencies, Ω, increase with moderate increase of the width of the instability zones. The same effects are observed for other in-plane edge loading cases also. The results in Fig. 12 can be explained by the fact that δ and γ are proportional to the cross-sectional area and the cross-sectional moment of inertia of the stiffener, respectively. Therefore, as γ increases, the rigidity of the stiffened plate increases and the plate becomes more stable.

A simply supported square plate with a central stiffener has also been analyzed with various ratios of cross-sectional area of the stiffener to that of the plate ($\delta = 0.05$, 0.1, 0.15, 0.2, 0.25) keeping fixed bending stiffness rigidity ($\gamma = 10$). The torsional inertia of the stiffeners has been neglected. The effects of stiffener area ratios of the stiffened plate on the principal dynamic stability region are studied and the results obtained are presented in Fig. 13. It is observed that the onset of instability appears earlier as δ is increased for a fixed value of γ. However, the width of instability regions remains unaffected.

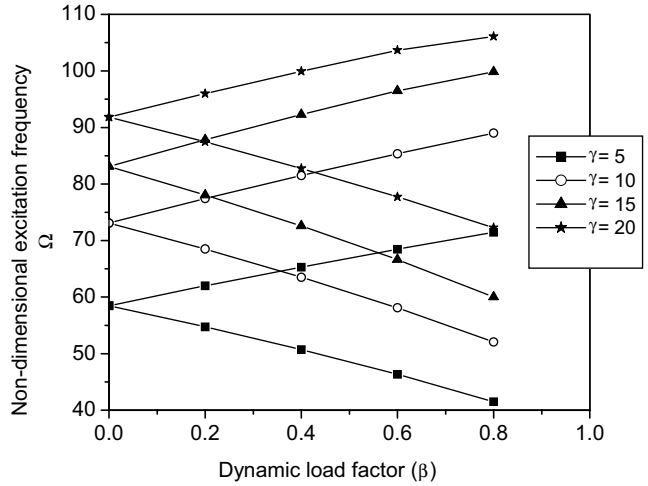

Fig. 12. Effect of γ on instability region of simply supported stiffened plate ($\delta = 0.1$) subjected to partial edge loading at centre ($\alpha = 0.2$, $c/b = 0.2$).

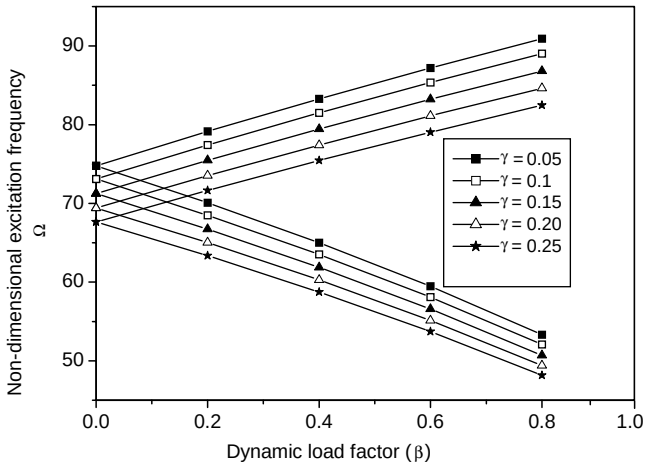

Fig. 13. Effect of δ on instability region of simply supported stiffened plate ($\gamma = 10$) subjected to partial edge loading at centre ($\alpha = 0.2$, $c/b = 0.2$).

4. Conclusion

The results from a study of the instability behaviour of stiffened plates subjected to non-uniform periodic in-plane compressive edge loading can be summarized as follows:

1. The instability regions are shifted to lower frequencies and become wider with the increase of static load factor showing a destabilizing effect on the dynamic stability behaviour of the stiffened plate.

2. The width of instability zones is reduced with the decrease in the value of c/b ratio for all loading cases. However, in higher range of β ($\geqslant 0.4$), the upper excitation frequency parameter of higher c/b ratio is found to be more compared to that corresponding to lower c/b ratio.
3. The onset of dynamic instability occurs at higher frequency for higher aspect ratio with wider instability regions.
4. If the cross-sectional dimensions of the stiffeners are the same, then the plate with more stiffeners has a smaller principal dynamic instability region.
5. The onset of instability occurs later with the addition of restraint at the edges.
6. The instability boundary frequencies, Ω, increase with moderate increase of the width of the instability zones when bending stiffness rigidity of the stiffener is increased for a fixed value of stiffener cross-sectional area. However, the result is reversed when ratio of stiffener cross-sectional area is increased for a fixed value of bending stiffness rigidity of the stiffener.

Appendix A. Nomenclature

a	plate dimension in longitudinal direction
b	plate dimension in the transverse direction
c	distance of concentrated load from bottom edge along y direction and also width of partial load (Fig. 1)
t	plate thickness
E, G	Young's and shear moduli for the plate material
υ	the Poisson ratio
b_S, d_S	web thickness and depth of an x-stiffener
ξ, η	non-dimensional element co-ordinate
A_S	cross-sectional area of the stiffener
I_S	moment of inertia of the stiffener cross-section about reference axis
q_r	vector of nodal displacement at rth node
$[D_P]$	rigidity matrix of plate
$[D_S]$	rigidity matrix of stiffener
$[K_e]$	elastic stiffness matrix of plate
$[K_S]$	elastic stiffness matrix of stiffener
$[M_P]$, $[M_S]$	consistent mass matrix of plate, stiffener
$[K_G]$	geometric stiffness matrix
$[N]_r$	matrix of a shape function of a node r
P_{cr}	critical buckling load
$P(t)$	in-plane load
P_S	static portion of P
P_t	amplitude of dynamic portion of P
α	static load factor
β	dynamic load factor
Ω	frequency of forcing function
U	upper excitation frequency parameter
L	lower excitation frequency parameter

References

[1] V.V. Bolotin, The Dynamic Stability of Elastic Systems, Holden-Day, San Francisco, 1964.
[2] K.S. Jagdish, The dynamic stability of degenerate systems under parametric excitation, Ingenieur-Archiv 43 (1974) 240–246.
[3] N. Yamaki, K. Nagai, Dynamic stability of rectangular plates under periodic compressive forces, Report of the Institute of High Speed Mechanics, Tohoku University, Japan, No. 32, 1975, pp. 103–127.
[4] J.M. Hutt, A.E. Salam, Dynamic instability of plates by finite element method, American Society of Civil Engineers Journal of Engineering Mechanics 3 (1971) 879–899.
[5] K. Takahasi, Y. Konishi, Dynamic stability of rectangular plate subjected to distributed in-plane dynamic force, Journal of Sound and Vibration 123 (1) (1988) 115–127.
[6] P.J. Deolasi, P.K. Datta, Parametric instability characteristics of rectangular plates subjected to localized edge compressing (compression or tension), Computer and Structures 54 (1995) 73–82.
[7] D.L. Prabhakar, P.K. Datta, Parametric instability characteristic of rectangular plates with localized damage subjected to in-plane periodic load, Computer and Structures 49 (1994) 825–836.
[8] S.A. Ambartsumyan, A.A. Khachaturian, On the stability and vibration of an anisotropic plate, Dokladi Akad SSR 1 (1960) 113–122 (in Russian).
[9] R.C. Duffield, N. Willens, Parametric resonance of rectangular plates, Journal of Applied Mechanics 39 (1972) 217–226.
[10] R.G. Merrit, N. Willens, Parametric resonance of skew stiffened plates, Journal of Applied Mechanics 40 (1973) 439–444.
[11] M. Mermertas, H.T. Belek, Dynamic stability of radially stiffened annular plates, Computer and Structures 40 (3) (1991) 651–657.
[12] C.L. Liao, C.R. Cheng, Dynamic stability of stiffened laminated composite plates and shells subjected to in-plane pulsating forces, Journal of Sound and Vibration 174 (3) (1994) 335–351.
[13] M. Mukhopadhyay, A. Mukharjee, Finite element buckling analysis of stiffened plates, Computer and Structures 34 (6) (1990) 795–803.
[14] A.H. Sheikh, M. Mukhopadhyay, Free vibration analysis of stiffened plates with arbitrary planform by the general spline finite strip method, Journal of Sound and Vibration 162 (1) (1993) 147–164.
[15] A. Mukherjee, M. Mukhopadhyay, Finite elements free vibration of eccentrically stiffened plates, Computer and Structures 30 (6) (1988) 1303–1318.
[16] O.C. Zienkiewicz, R.L. Taylor, The Finite Element Method, 4th Edition, McGraw-Hill, New York, 1989.
[17] R.B. Corr, A. Jenning, A simultaneous iteration algorithms for symmetric eigenvalue problem, International Journal for Numerical Methods in Engineering 10 (1976) 647–663.
[18] A.W. Leissa, E.F. Ayoub, Vibration and buckling of simply supported rectangular plate subjected to a pair of in-plane concentrated forces, Journal of Sound and Vibration 127 (1988) 155–171.
[19] C.J. Brown, Elastic stability of plates subjected to concentrated loads, Computer and Structures 33 (5) (1989) 1325–1327.
[20] S.P. Timoshenko, J.M. Gere, Theory of Elastic Stability, 2nd Edition, McGraw-Hill, New York, 1961.